

VU Research Portal

Tracking motor unit action potentials in the tibialis anterior during fatigue

Beck, R.B.; O'Malley, M.J.; Stegeman, D.F.; Houtman, C.J.; Connolly, S.; Zwarts, M.J.

published in

Muscle and Nerve
2005

DOI (link to publisher)

[10.1002/mus.20375](https://doi.org/10.1002/mus.20375)

document version

Publisher's PDF, also known as Version of record

[Link to publication in VU Research Portal](#)

citation for published version (APA)

Beck, R. B., O'Malley, M. J., Stegeman, D. F., Houtman, C. J., Connolly, S., & Zwarts, M. J. (2005). Tracking motor unit action potentials in the tibialis anterior during fatigue. *Muscle and Nerve*, 32, 506-14.
<https://doi.org/10.1002/mus.20375>

General rights

Copyright and moral rights for the publications made accessible in the public portal are retained by the authors and/or other copyright owners and it is a condition of accessing publications that users recognise and abide by the legal requirements associated with these rights.

- Users may download and print one copy of any publication from the public portal for the purpose of private study or research.
- You may not further distribute the material or use it for any profit-making activity or commercial gain
- You may freely distribute the URL identifying the publication in the public portal ?

Take down policy

If you believe that this document breaches copyright please contact us providing details, and we will remove access to the work immediately and investigate your claim.

E-mail address:

vuresearchportal.ub@vu.nl

ABSTRACT: New surface electromyogram (SEMG) techniques offer the potential to advance knowledge of healthy and diseased motor units. Conduction velocity (CV) estimates, obtained from indwelling electrodes, may provide diagnostic information, but the standard method of CV estimation from SEMG may be of only limited value. We developed a motor unit (MU) tracking algorithm to extract motor unit conduction velocity (MUCV) and motor unit action potential (MUAP) amplitude estimates from SEMG. The technique is designed to provide a noninvasive means of accessing fatigue and recruitment behavior of individual MUs. We have applied this MU tracking algorithm to SEMG data recorded during isometric fatiguing contractions of the tibialis anterior (TA) muscle in nine healthy subjects, at 30%–40% maximum voluntary contraction (MVC). The results reveal that MUCVs and MUAP amplitudes of individual MUs can be estimated and tracked across time. Time-related changes in the MU population may also be monitored. Thus, the SEMG technique employed provides insight into the behavior of the underlying muscle at the MU level by noninvasive means.

Muscle Nerve 32: 506–514, 2005

TRACKING MOTOR UNIT ACTION POTENTIALS IN THE TIBIALIS ANTERIOR DURING FATIGUE

REBECCA B. BECK, PhD,¹ MARK J. O'MALLEY, PhD,¹ DICK F. STEGEMAN, PhD,²
CAROLINE J. HOUTMAN, PhD,³ SEAN CONNOLLY, MD,⁴ and MACHIEL J. ZWARTS, MD, PhD²

¹ Department of Electronic and Electrical Engineering, University College Dublin, Dublin, Ireland

² Department of Clinical Neurophysiology, Institute of Neurology, Radboud University Nijmegen Medical Center, Nijmegen, The Netherlands

³ Program for Sport Sciences, Faculty of Social Sciences and Technology Management, Norwegian University of Science and Technology, Trondheim, Norway

⁴ Department of Clinical Neurophysiology, St. Vincent's University Hospital, Dublin, Ireland

Accepted 11 April 2005

The conduction velocity (CV) of a muscle fiber action potential is intimately linked to the excitability of the muscle fiber membrane. CV estimates can therefore provide useful information about the pathophysiological state of the muscle. CV estimates may be of diagnostic value for, among other conditions, hypokalemic periodic paralysis,^{34,35} amyotrophic lateral sclerosis,³⁶ inflammatory myopathy,⁷ and Duchenne muscular dystrophy.^{1,9,10,17,31,32} The success of CV as a diagnostic or investigative tool is dependent on the recording technique, the experimental protocol, and the accuracy of the method of CV estimation.

The typical approach to CV estimation from the surface electromyogram (SEMG) is to determine the time delay for an epoch of data (usually 0.5 to 2 s in duration) to propagate between two spatially displaced surface electrode pairs. This results in a single estimate, referred to here as the global-CV estimate. The SEMG generated from a voluntarily contracting muscle comprises the combined electrical activity of a number of different motor units (MUs) with different fiber types, varying sizes and relative locations, different fatigue and recruitment patterns, and different motor unit conduction velocities (MUCVs) and firing statistics. Therefore a single, global-CV estimate may be of limited value. However, the noninvasive nature of SEMG provides many advantages over its invasive counterpart, including the ability to record signals during voluntary fatiguing contractions. The analysis of fatiguing contractions may provide a means by which to: (1) monitor the electrical behavior of different MU types on the basis of CV values and recruitment-force/time relationships; (2) detect MU fatigue by way of changes in CV and amplitude estimates, and alterations in the MU pop-

Abbreviations: CV, conduction velocity; MU, motor unit; MUAP, motor unit action potential; MUCV, motor unit conduction velocity; MVC, maximum voluntary contraction; NDD, normal double differential; RMS, root mean square; SEMG, surface electromyogram; TA, tibialis anterior

Key words: fatigue; motor unit action potential amplitude; motor unit conduction velocity; motor unit recruitment; surface electromyogram

Correspondence to: M. O'Malley; e-mail: mark.omalley@ucd.ie

© 2005 Wiley Periodicals, Inc.

Published online 22 June 2005 in Wiley InterScience (www.interscience.wiley.com). DOI 10.1002/mus.20375

ulation; and (3) identify pathological situations owing to abnormalities in CV or amplitude values, numbers of detected MUs, or recruitment behavior. In recognition of the benefits of SEMG recordings, more advanced methods of CV estimation from SEMG have been developed.^{5,14,18,21,24} One approach is to estimate velocities of individual peaks in the SEMG signal.^{5,18,21,24} Houtman et al.²¹ used such an approach in a study of SEMG from isometric, sustained, fatiguing contractions of the tibialis anterior (TA) in five healthy subjects. Peak velocity distributions were determined for individual data epochs and interpreted as illustrating the fatigue of type I MUs followed by the recruitment and subsequent fatigue of type II MUs.

The aims of the current study were to determine, firstly, whether the activity of individual MUs (as opposed to that of individual peaks) may be observed from the SEMG and, secondly, whether fatigue and recruitment patterns of individual MUs may be revealed by analyzing the SEMG recorded during sustained fatiguing contractions. In order to achieve these aims, SEMG signals were recorded from nine healthy volunteers during sustained fatiguing contractions of the TA. These data were analyzed using our recently developed MU tracking algorithm, the performance of which has previously been assessed on simulated SEMG signals.⁵ The MU tracking algorithm results in the extraction of representative values for the amplitudes and CVs of individual motor unit action potentials (MUAPs), which are then tracked across time.

MATERIALS AND METHODS

Subjects and Protocol. Approval was obtained from the medical ethical committee of the Radboud University Nijmegen Medical Center. Nine healthy volunteers (six men and three women), with a mean age of 37 years, participated in this study. Subjects sat reclined on a bench with a vacuum cushion supporting their left thigh and knee such that the quadriceps muscle was relaxed and an angle of $\sim 90^\circ$ was achieved at the ankle.^{13,21} Their left foot was strapped into a rigid plate attached to a force transducer. The SEMG was gathered using a high-density surface electrode array consisting of 32 gold-plated electrodes (four columns and eight rows). The electrodes were 1.52 mm in diameter and had serrated contact surfaces.⁸

The skin was abraded and a small quantity of electrode gel was applied and allowed to be absorbed; excess gel was removed before attaching the electrode grid. The electrodes were placed parallel to the underlying muscle fibers on the distal third of

the TA. The distal portion was chosen as the end-plates of this muscle are known to be scattered along the superficial layers, with higher densities in the proximal and mid-portions.² The correct alignment of the electrodes and the avoidance of end-plate activity were made possible by the online visual feedback of the acquisition software, developed in-house by J. P. van Dijk, Nijmegen, The Netherlands. The alignment of the electrodes could be verified by analyzing the cross-correlation coefficients of SEMG signals obtained from consecutive bipolar electrode pairs, in addition to visually monitoring the propagation of MUAPs from the most proximal to the most distal electrode. This ability to monitor propagating MUAPs also aided the detection of end-plate activity. The electrode-skin contact impedance was determined for each electrode by applying a 20-mV (peak-to-peak) 62.5-Hz square-wave signal over a 1-M Ω resistor in series with the single grid-electrode and the common mode sensor (the resistance of which was assumed to be small relative to the grid-electrode). The electrode-skin contact was considered acceptable when the majority of grid-electrodes had impedances below 300 k Ω .

Subjects performed one or two short test contractions to help them focus on activating only the TA when pulling against the foot-strap, keeping the muscles of the upper thigh and foot as relaxed as possible. The maximum voluntary contraction (MVC) of each subject was determined by taking the maximum of three trial contractions. The trials were separated by at least 1 min and lasted 3 to 5 s. Verbal encouragement was given each time. After a rest period of at least 5 min, subjects were asked to sustain an isometric contraction at 30% MVC until exhaustion. Two subjects (5 and 7) repeated this experiment at 40% MVC due to particularly low MVC values (Table 1). The force output was displayed on a computer in front of the subject. The target force and $\pm 5\%$ deviation from this force were clearly illustrated on the display. The subject was instructed to maintain the force within these 5% deviation margins. The start of the contraction was defined as the point at which the mean force exceeded 90% of the target force for at least 3 s, and the end was the point at which the mean force was less than 90% of the target force for at least 3 s. The endurance time for each subject was defined as the time between the start and end points.

Data Acquisition. The force and SEMG data were gathered on separate computers but synchronized using a time-code signal. One input channel from the 4×8 SEMG electrode grid was used as the

Table 1. Summary of results for all subjects.*

Subject	MVC (N)	Duration (s)	No. MUs		MUCV		MUAP		Time (%)		
			Total	Mean	(m/s)	% Change	(μ V)	% Change	Detected	Start <50%	End <50%
1	164	374	11	5	3.00 (0.1)	-7.0	1,155 (74)	-5.9	47	100	45
2	161	367	16	8	3.49 (0.1)	0.6	1,524 (81)	-3.8	46	75	13
3	131	520	11	5	2.33 (0.1)	-5.8	579 (82)	-19.1	41	82	9
4	208	922	10	3	3.49 (0.1)	0.0	572 (37)	-3.6	38	50	10
5 [†]	85	589	16	6	3.75 (0.2)	1.1	474 (37)	14.1	34	75	31
6	143	400	12	5	3.01 (0.2)	-3.4	998 (85)	-5.8	36	75	17
7 [†]	84	222	12	7	3.71 (0.1)	1.8	1,631 (99)	-5.1	57	83	8
8	91	862	14	6	3.12 (0.1)	4.0	775 (62)	-3.0	42	93	36
9	137	373	18	6	3.02 (0.1)	0.6	267 (22)	-7.6	31	61	17
Mean	134	514	13	6	3.21 (0.1)	-0.9	886 (64)	-4.44	41	77	21

*Two subjects, indicated with daggers, performed the fatiguing contractions at 40% MVC; all others sustained 30% MVC contractions. The number of detected motor units (No. MUs) for each subject is summarized by 'Total', the total number of MUs detected during the contraction, and 'mean', the mean number MUs detected at any one instant. The median (standard deviation) of the MUCV (and MUAP amplitude) is determined for each MU for each subject. The medians of these values are shown for each subject. '% change' is the median of the percent changes calculated for each MU for that subject. Three parameters relating to time are provided. 'Detected' is the median of the percentages of the total contraction time for which the activities of individual MUs are detected. 'Start <50%' provides the percentage of the total number of detected MUs for that subject for which activity is detected within the first half of the total contraction duration. 'End <50%' provides the percentage of the total number of detected MUs for which activity appears to cease within the first half of the contraction time.

synchronization channel. Thirty-one monopolar SEMG signals were recorded. The monopolar signals were amplified, band-pass filtered (3–800 Hz), and subsequently analog-to-digital converted using a 64-channel amplifier system at a sampling rate of 4 kHz (Mark 6, Biosemi, Amsterdam, The Netherlands). A common reference gold-plated cup-electrode, with a diameter of 1 cm, was filled with electrode gel and taped to the skin, remote from the grid, on the patella. All grid-electrodes were referenced to that electrode (monopolar recording). Another similar cup-electrode, the common mode sensor, was placed near the reference to accommodate the driven-right-leg amplifier configuration, a technique designed to reduce noise and increase patient safety.³⁰

Spatially filtered SEMG signals, to enable increased selectivity, were derived using the normal double differential (NDD) configuration.¹² The peak of a resultant MUAP from an NDD SEMG signal (as opposed to the zero-crossing as would be the case for bipolar signals) is expected to correspond to the instant at which the MUAP passes the center of the electrode configuration, thus enhancing the precision of MUCV estimation.¹¹ An inter-electrode distance of 6 mm was used in each NDD configuration with an intersignal distance (i.e., distance between the two NDD signals used for CV estimation) of 12 mm.³ Two consecutive NDD SEMG signals, 12 mm apart, were selected for each subject. The selection criteria required that the signals be situated far from any visible end-plate activity, detected from visual inspection of the bipolar data. The selected signals also had high cross-correlation coefficients (indicative of good quality data), and

low mean global-CV values. Signals with low mean global-CV values were favored as the effects of interference or end-plate activities, i.e., nonpropagating components, may cause the global-CV estimate to be biased towards higher values.

Data Analysis. The data from each subject were analyzed in 2-s epochs throughout the fatiguing contraction. The global-CV estimate, determined using the phase-shift method,²⁸ and the root-mean square (RMS) value were stored for each epoch. The MU tracking algorithm was then applied, resulting in MUAP amplitudes and MUCV values being tracked across time. Throughout this article, the results obtained from the MU tracking algorithm will be referred to as MU traces, and the velocity and amplitude values they represent as MUCVs and MUAP amplitudes. However, some liberty is being taken as these traces are approximations of the underlying activity, and should be viewed as such. A brief overview of the MU tracking algorithm is included here. A full description can be found elsewhere.⁵

The MU tracking algorithm can be broken down into three parts. The first part involves the processing of the raw SEMG data in 2-s epochs. Signal peaks exceeding a threshold value are identified and their associated amplitudes and velocities calculated, resulting in distributions of peak amplitudes and peak velocities being determined per epoch. These distributions are analyzed in the second part of the MU tracking algorithm. A clustering procedure is performed whereby peaks with similar amplitudes and velocities are identified. The times of occurrence of each peak are also taken into account prior to a peak

being granted membership of a cluster. Every firing of a particular MU may not be detected in a given epoch, due to the probable occurrence of MUAP interference, or for peaks close to the detection threshold, subtle reductions in amplitude. Therefore, no attempt is made to extract entire MUAP trains or accurate firing rate information, but rather interpulse interval information is used to verify that similar peaks could realistically belong to the same MU (based on the assumption that the interpulse interval may not be less than 20 ms, i.e., a maximum MU firing rate of 50 Hz). The member peaks of a cluster are expected to represent multiple sample firings from the same MUAP train. Therefore, MUAP amplitudes and MUCVs are derived from the centers of gravity of each cluster of peak amplitudes and peak velocities. It is assumed that peaks which are not assigned to a cluster do not represent an individual MUAP, but rather that these peaks have arisen from the interference of two or more MUAPs or are for some other reason spurious. Such peaks are rejected at this stage of the algorithm. The final part of the algorithm tracks the activities of the cluster centers, assumed to represent individual MUs, across epochs. A set of MUCVs and MUAP amplitudes is calculated from the 10 previous epochs using a moving average. Tolerances are determined between each cluster center (representing a MU) in the current epoch and each point in the moving average set. The union with the lowest tolerance is accepted. If a particular cluster center in the current epoch is not matched with any points from the moving average set, i.e., all tolerances are greater than a threshold level, then this value is assigned to a new MU. This process is repeated for all epochs resulting in MU traces of both MUAP amplitudes and MUCVs. These MU traces are then analyzed, some with similar values may be merged, and others with sparse entries and cluster centers derived from small clusters, are rejected. Piecewise cubic Hermite interpolation is performed on each of the traces to account for possible missing data, before applying a smoothing third-order digital filter.

RESULTS

Peak Clustering and Analysis. Two 2-s segments of the NDD SEMG signals from subject 3 are shown in Figure 1 for epochs occurring early (A) and late (B) in the contraction period (see time scales below figures). The corresponding peak amplitude and velocity values are given in Figure 2. These distributions of peak values indicate the increase in signal amplitude, seen by comparing Figure 1A and B, but also a marked increase in

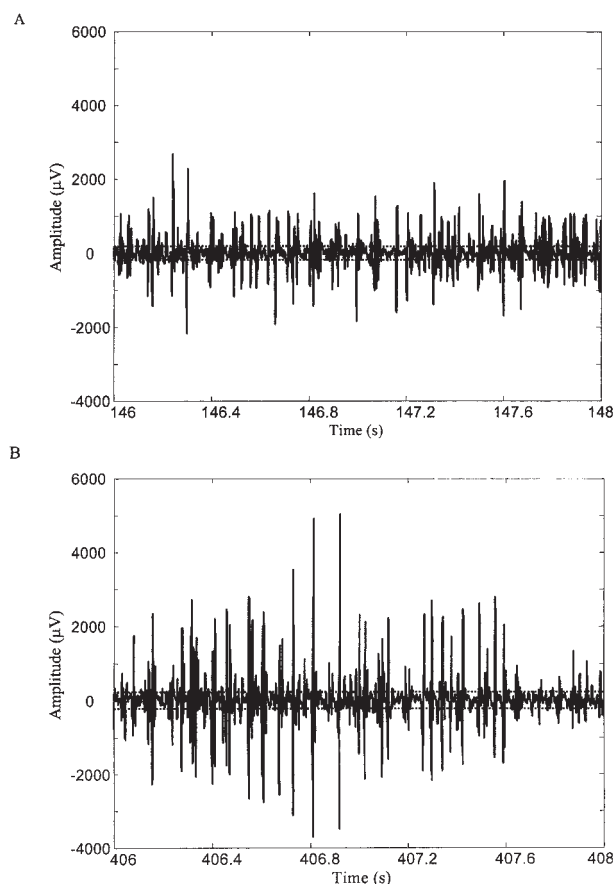


FIGURE 1. Two 2-s extracts of NDD SEMG data from subject 3, taken 146 s (A), and 406 s (B) after the start of the contraction. The horizontal dotted lines represent the peak-detection threshold applied.

the range of peak velocity values. The cluster centers, obtained in the analysis, are marked by the heavy diamonds and represent MUCV and MUAP amplitude values, i.e., the centers of gravity of the peak velocities and peak amplitudes for each cluster.

Tracking MUAP Amplitudes and MUCVs. Sample results from two subjects (3 and 6) are shown in Figures 3 and 4. In both cases, the first plot (A) illustrates the approximated MUCV estimates for individual MUs; the global-CV estimate is also included (heavy solid line). An initial relatively smooth decrease in the global-CV is followed by a subsequent increase with increasing variability. This is particularly marked in the results of subject 3 (Fig. 3A). The corresponding MUAP amplitude values are shown in the lower plots (B); the heavy solid line is the maximum RMS value of the two NDD SEMG signals used for CV estimation. The times for which the activity of individual MUs is detected and assumed to indicate the period of activity of that MU,

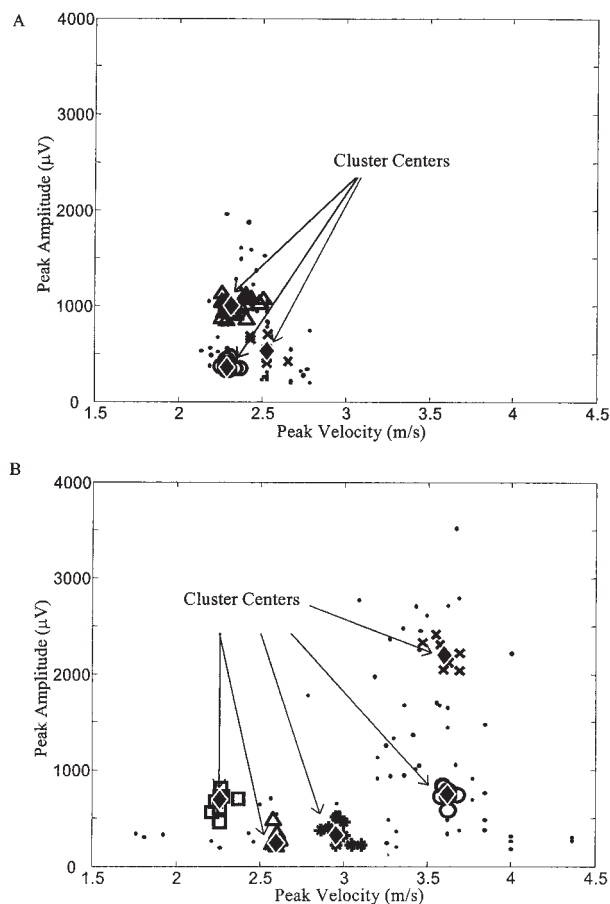


FIGURE 2. (A) Peak velocity and amplitude values calculated for the data epoch shown in Figure 1A. (B) Peak velocity and amplitude values calculated for the data epoch shown in Figure 1B. Peaks belonging to a particular cluster are represented by a common symbol, e.g., \circ , \times , $*$, \square , \triangle . The heavy diamonds (with white outline) illustrate the center of each cluster. The dots represent the peaks that have not been assigned to a cluster.

can be clearly seen from these plots. Due to the larger relative differences in amplitude values, as opposed to conduction velocity values of the MU traces, the activity of individual MUs may often be seen more easily using the MUAP amplitude plots. The results from the tracking phase of the algorithm for subject 3 revealed that the clusters identified in Figure 2 were found to belong to different MUs.

A summary of the results from all subjects is provided in Table 1. The total number of MUs detected per subject is provided, as is the number of MUs detected at a given instant. This value is calculated by determining the number of MUs detected, i.e., the number of active MU traces, at each instant. The mean of these values is then determined, providing an estimate of the average number of MUs detected concurrently for each subject. Table 1 also provides an indication of the time-dependent trends in MUCV and

amplitude values (% change). Due to the local variability of many of the traces, a direct estimate of the rate of change of a particular trace was thought to be less informative than the parameter chosen (% change, Table 1), which is determined by estimating the percentage change in MUCV and MUAP amplitudes values between the mean of the first five and that of the last five estimates for each MU trace. Details are also provided regarding timing characteristics of the MU activity for each subject.

DISCUSSION

Tracking MUAP Amplitudes and MUCVs. Subjects were, in general, able to maintain a smooth force output in the initial stages of the contraction. This

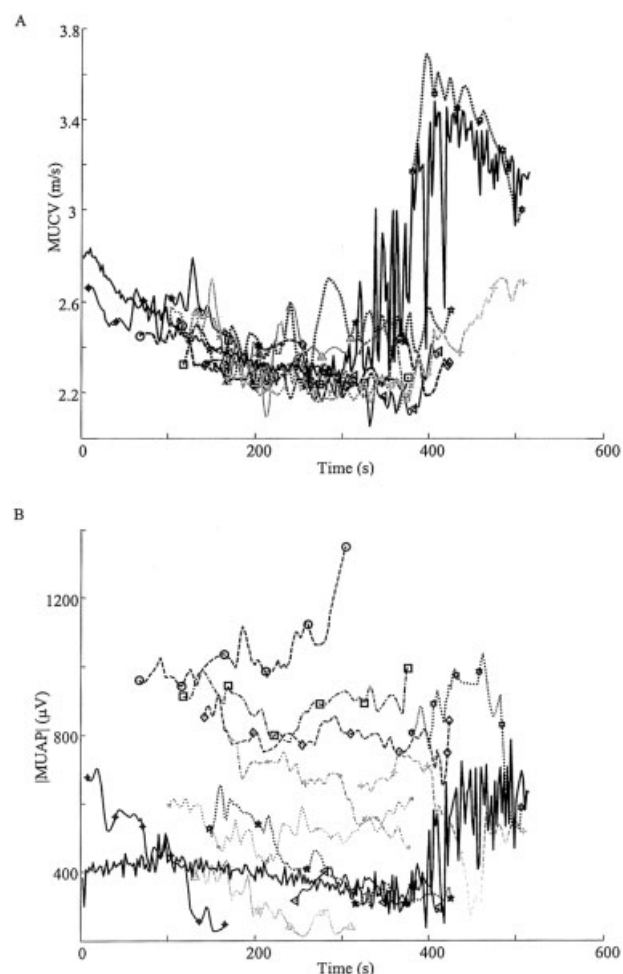


FIGURE 3. Tracking MUCV (A) and MUAP amplitude (B) values during the fatiguing contraction of subject 3. Symbols and shading is used to identify individual MUs. The same symbols and shading are used on the MUCV and the corresponding MUAP amplitude traces for a given MU. The heavy solid line in (A) represents the global-CV value; in (B), it represents the maximum RMS value of the two NDD SEMG signals.

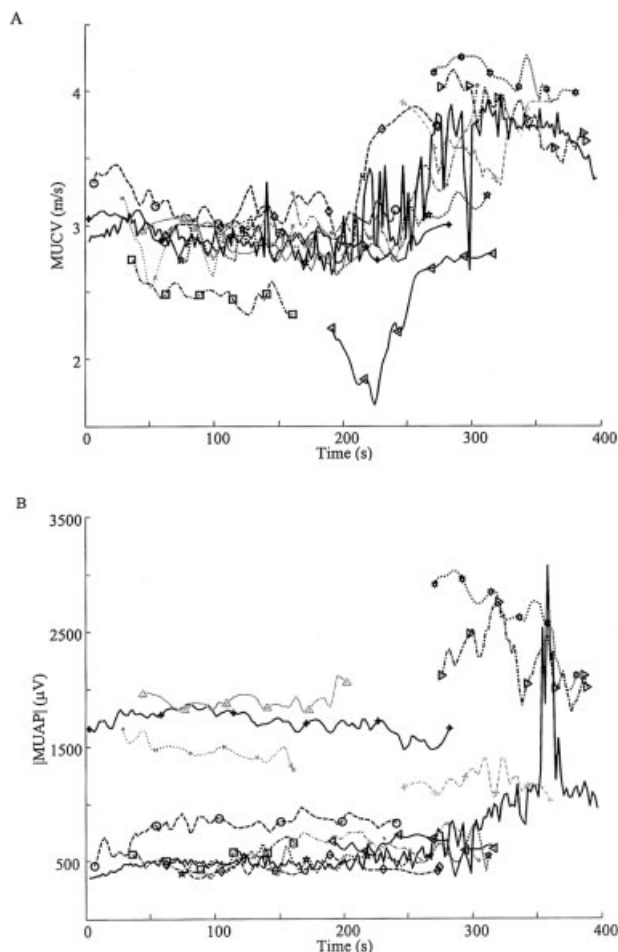


FIGURE 4. MUCV (**A**) and MUAP amplitude (**B**) values for subject 6. See legend of Figure 3 for further details.

was associated with a relatively smooth decrease in the mean global-CV estimate, which in turn was associated with a narrow range of MUCV values as revealed in the results from the MU tracking algorithm. As the contraction progressed and it became increasingly difficult for the subject to sustain the target force, the variability of the global-CV estimate increased in most subjects. This increased variability of the global-CV was often coupled with a wider range of MUCV values (Figs. 3A and 4A). Such an increase in the range of MUCV values may be indicative of changes in the make-up of the MU population resulting from the sustained effort, i.e., the presence of MUs with different MUCV values possibly due to MUs of the same type in differing degrees of fatigue, or to recruitment of MUs of different type and hence different inherent MUCV values.

The frequently reported fatigue-induced increase in SEMG amplitude^{27,29} was observed in all subjects in this study. A number of factors have been

proposed in the literature to explain this amplitude increase, including: MU recruitment and a resultant increasing presence of larger-amplitude type II MUs; the inverse relationship between MUCV and signal amplitude estimates such as RMS and the average rectified value; and changes in MU firing rates and synchronization.^{6,25,26,29,33} Two interesting insights in relation to the recruitment aspect of these explanations arise from the current analysis. First, a marked time-dependent increase in peak amplitudes was observed, but the amplitudes of cluster centers or MUAPs increased to a lesser extent. It therefore appears that the time-dependent increase in signal amplitude may frequently be accentuated by large peak amplitudes arising from MUAP interference to a level greater than can be explained by the amplitudes of the MUAPs alone. (Relating back to the above explanations for the increase in SEMG amplitude, this apparent increase in MUAP interference could be a consequence of increases in MU firing rates or synchronization.)

The second point relates to the assumption that type II MUs are responsible for the time-dependent increase in amplitude. It can be seen from these results, and those of Houtman et al.²¹ that high-amplitude peaks are often, though not exclusively, associated with higher velocity values, and that the slightly faster, larger, later-recruited type II MUs may in fact have relatively low amplitudes (Fig. 2). Of the five MUs detected in the epoch shown in Figure 2B, two can be seen to share the maximum velocity of approximately 3.6 m/s. Though these cluster centers, or MUs, share a similar velocity value, one has a large amplitude—as might be expected from an assumption of an amplitude–velocity dependency—but the amplitude of the other is almost identical to that of a MU with a velocity of only 2.3 m/s. Such variations in the relationships between amplitude and velocity imply that, depending on the density of type II fibers in the superficial layers of the muscle (roughly 25% of muscle fibers in the superficial layers of the TA are type II^{22,16}), the activity of a later recruited type II MU may not necessarily contribute more to the increase in SEMG amplitude than the earlier recruited MUs.

One further point in relation to the changes in amplitude can be mentioned. Some MUAP amplitude traces can be seen to increase with time (Figs. 3B and 4B). A possible explanation for this is that decreasing velocities, when coupled to an increased duration of the intracellular action potential, will increase amplitude.³³

The timings of the start and end of the detection period for individual MUs (Figs. 3 and 4) and groups

of MUs (Table 1) have been provided. On average, the activity of 13 MUs was monitored in each subject, with each MU being active for a mean duration of 41% of the total contraction time (Table 1). The timings for which the activities of MUs are detected, start <50%, end <50%, may be interpreted as indicating the degree of recruitment and de-recruitment from the MUs pool for individual subjects during the course of the contraction. Such information is of great potential value both physiologically and diagnostically. The interpretation of a "lost peak" as the moment of MU derecruitment has to be made with care. Theoretically, signal quality changes or increased levels of interference can also cause such a loss. Although these results are preliminary, they corroborate those reported elsewhere, both in terms of the time-dependent behavior of active MUs in the TA¹³ and in terms of the recruitment patterns of MUs during sustained, moderate-force contractions of the TA.^{19–21} Hägg¹⁵ claims that "the hypothesis of successive additional recruitment of new unfatigued MUs to maintain a constant force output is old. . . . However, so far no one has been able to show convincing EMG evidence for the existence of this phenomenon." The results of the current study, and also Houtman et al.,²¹ could be interpreted as providing SEMG evidence of its existence. However, though the MU tracking algorithm has been shown previously to work successfully for selective simulated SEMG signals,⁵ and the results from the current application reveal that this novel approach provides a new means by which to monitor the time-dependent activity of individual MUs from the SEMG, this technique is as yet at an early stage of development, and is not without its limitations. A few considerations are discussed below (see Beck et al.⁵ for more detailed discussion).

Data Analysis and Interpretation Challenges. Cluster sizes are defined for each data epoch by iteratively analyzing the data with different parameter values and automatically selecting the cluster set which has the most favorable validation index (derived from the ratio of the between-cluster distances to within-cluster distances). However, there is an inherent trade-off between cluster sizes and the number of clusters detected. The impact of such a trade-off in terms of SEMG analysis is that small cluster sizes may result in larger numbers of MUs being reported. This potential over-representation of some data epochs may be reduced (but not necessarily eliminated) by the tracking process, which by attempting to track the activity of consistently represented MUs, effectively distills the MU population to a core group.

As the contraction progresses and more MUs are recruited, it is inevitable that the SEMG signal will become more crowded and the likelihood of MUAP interference will increase, thereby reducing the number of signal peaks which represent unadulterated MUAPs and as a result making the process of MU identification (via cluster definition) and tracking of MU activity more challenging. In addition, the time-dependent increase in RMS values of the SEMG signals could lead to the loss of detection of lower-amplitude MUAPs in the later part of a contraction. A number of steps can be taken to deal with these challenges.

First, selective surface electrodes can be used resulting in clear signals with less MUAP interference due to the activity of a smaller number of MUs being recorded. An NDD electrode configuration was used in this study. Second, even when selective surface electrodes are used, some MUAP interference is still likely to occur. The velocity and amplitude of a given MUAP changes in an unpredictable manner when it interferes with another MUAP.⁴ It is likely therefore that the velocity and amplitude of a peak, resulting from the interference of two or more MUAPs, will not match the corresponding velocities and amplitudes of any of the original MUAPs. The influence of MUAP interference is reduced during the clustering process as an interference peak would not be granted membership of any of the parent clusters owing to it not satisfying the required velocity, amplitude, and timing criteria. Third, to limit the possibility that an increase in the amplitude of the SEMG would reduce the ability to detect the activity of lower amplitude MUAPs, the same peak-detection threshold is used throughout the contraction. The peak-detection threshold for each subject is defined as 60% of the mean RMS value for the first 10 epochs, e.g., 20 s, of the contraction. As a result, the amplitude of the smallest detected peak may be the same at the end of the contraction as at the beginning. Despite these precautions, the possibility that the activity of some MUs may become overshadowed by that of others, and hence lost to our detection, cannot be excluded.

We do not have a gold standard against which to compare our results. For this reason, the analysis has been performed previously on simulated data⁵ in order to enable an informed assessment of the results. Such a luxury is not available when dealing with experimental data analysis. One proposition may be to use simultaneous needle EMG recording as a means of validating the results from SEMG analysis. However, this approach may not provide the desired gold standard as it would be difficult to

guarantee that both the surface and needle electrodes record from the same MU. The amplitudes, and probably waveforms, of the recorded MUAPs would differ between the two recording techniques; it would not be a practical means by which to evaluate the MUCV values due to the difficulty of estimating MUCV invasively during voluntary contractions; and finally the needle electrodes would likely record from fewer MUs, and hence would not provide enough information to validate the SEMG analysis. One way of increasing the robustness of the technique is the addition of more spatial information and especially including electrodes in the direction perpendicular to the muscle fiber direction.²³ This may be particularly beneficial in the case of significant MUAP interference.

In conclusion, we propose that the technique used in this analysis—of associating signal peaks based on their velocities, amplitudes, and times of occurrence, in order to estimate the behavior of individual MUs—provides a means of investigating changes in muscle activation at the MU level, which, though arguably not as precise as single MUCV estimation by multielectrode needle EMG techniques, is more precise than the standard SEMG techniques, e.g., resulting in a global-CV estimate. The results reveal that the activity and, hence, fatigue and recruitment behavior, of many individual MUs may be accessed in a noninvasive manner, though the issue of derecruitment still remains problematic. Nonetheless, this technique could prove to be an interesting investigative tool for the analysis of fatigue and recruitment phenomenon in both healthy and pathologic muscle.

This research was presented in part at: The Bioengineering in Ireland Conference 10, January 2004, Limerick, Ireland; The British Society of Clinical Neurophysiology, March 2004, Newcastle, United Kingdom; Quantitative EMG Congress, June 2004, Nijmegen, The Netherlands; and The International Society of Electromyography and Kinesiology, June 2004, Boston, Massachusetts. This work was partly funded by a traveling scholarship awarded by the National University of Ireland.

REFERENCES

- Al Ani FS, Hamdan FB, Shaikhly KI. In situ measurements of muscle fiber conduction velocity in Duchenne muscular dystrophy. *Saudi Med J* 2001;22:259–261.
- Aquiloni SM, Askmark H, Gillberg PG, Nandedkar S, Olson Y, Stalberg E. Topographical localization of motor endplates in cryosections of whole human muscles. *Muscle Nerve* 1984;7:287–293.
- Beck RB, O'Malley M, Van Dijk JP, Nolan P, Stegeman DF. The effects of bipolar electrode montage on conduction velocity estimation from the surface electromyogram. *J Electromyogr Kinesiol* 2004;14:505–514.
- Beck RBJ. Conduction velocity estimation from the surface electromyogram. Ph.D. Thesis, University College Dublin, Ireland, 2003.
- Beck RBJ, Houtman CJ, Stegeman DF, O'Malley MJ. A technique to track individual motor unit action potentials in surface EMG by monitoring their conduction velocities and amplitudes. *IEEE Trans Biomed Eng* 2005;52:622–629.
- Bigland-Ritchie B, Woods JJ. Changes in muscle contractile properties and neural control during human muscular fatigue. *Muscle Nerve* 1984;7:691–699.
- Blijham PJ, Hengstman GJ, Ter Laak HJ, Van Engelen BG, Zwarts MJ. Muscle-fiber conduction velocity and electromyography as diagnostic tools in patients with suspected inflammatory myopathy: a prospective study. *Muscle Nerve* 2004;29:46–50.
- Blok JH, Van Dijk JP, Drost G, Zwarts MJ, Stegeman DF. A high-density multichannel surface electromyography system for the characterization of single motor units. *Rev Sci Instrum* 2002;73:1887–1897.
- Chino N, Noda Y, Oda N. Conduction study in human muscle fibers in situ—a useful technique for diagnosing myopathies. *Electroencephalogr Clin Neurophysiol* 1984;58:513–516.
- Cruz MA, Lopez Terradas JM. Conduction velocity along muscle fibers in situ in Duchenne muscular dystrophy. *Arch Phys Med Rehabil* 1990;71:558–561.
- Disselhorst-Klug C, Rau G, Schmeer A, Silny J. Non-invasive detection of the single motor unit action potential by averaging the spatial potential distribution triggered on a spatially filtered motor unit action potential. *J Electromyogr Kinesiol* 1999;9:67–72.
- Disselhorst-Klug C, Silny J, Rau G. Improvement of spatial resolution in surface-EMG: a theoretical and experimental comparison of different spatial filters. *IEEE Trans Biomed Eng* 1997;44:567–574.
- Farina D, Arendt-Nielsen L, Merletti R, Graven-Nielsen T. Assessment of single motor unit conduction velocity during sustained contractions of the tibialis anterior muscle with advanced spike triggered averaging. *J Neurosci Methods* 2002;115:1–12.
- Farina D, Fortunato E, Merletti R. Noninvasive estimation of motor unit conduction velocity distribution using linear electrode arrays. *IEEE Trans Biomed Eng* 2000;47:380–388.
- Hägg GM. Interpretation of EMG spectral alterations and alteration indexes at sustained contraction. *J Appl Physiol* 1992;73:1211–1217.
- Henriksson-Larsen KB, Lexell J, Sjöström M. Distribution of different fibre types in human skeletal muscles. I. Method for the preparation and analysis of cross-sections of whole tibialis anterior. *Histochem J* 1983;15:167–178.
- Hilfiker P, Meyer M. Normal and myopathic propagation of surface motor unit action potentials. *Electroencephalogr Clin Neurophysiol* 1984;57:21–31.
- Hogrel JY, Duchene J. Motor unit conduction velocity distribution estimation: assessment of two short-term processing methods. *Med Biol Eng Comput* 2002;40:253–259.
- Houtman CJ, Heerschap A, Zwarts MJ, Stegeman DF. pH heterogeneity in tibial anterior muscle during isometric activity studied by (31)P-NMR spectroscopy. *J Appl Physiol* 2001;91:191–200.
- Houtman CJ, Heerschap A, Zwarts MJ, Stegeman DF. An additional phase in PCr use during sustained isometric exercise at 30% MVC in the tibialis anterior muscle. *NMR Biomed* 2002;15:270–277.
- Houtman CJ, Stegeman DF, Van Dijk JP, Zwarts MJ. Changes in muscle fiber conduction velocity indicate recruitment of distinct motor unit populations. *J Appl Physiol* 2003;95:1045–1054.
- Johnson MA, Polgar J, Weightman D, Appleton D. Data on the distribution of fibre types in thirty-six human muscles. An autopsy study. *J Neurol Sci* 1973;18:111–129.
- Kleine BU, Blok JH, Oostenveld R, Praamstra P, Stegeman DF. Magnetic stimulation-induced modulations of motor unit firings extracted from multi-channel surface EMG. *Muscle Nerve* 2000;23:1005–1015.
- Lange F, Van Weerden TW, Van Der Hoeven JH. A new surface electromyography analysis method to determine

- spread of muscle fiber conduction velocities. *J Appl Physiol* 2002;93:759–764.
25. Linssen WH, Stegeman DF, Joosten EM, van't Hof MA, Binkhorst RA, Notermans SL. Variability and interrelationships of surface EMG parameters during local muscle fatigue. *Muscle Nerve* 1993;16:849–856.
 26. Lowery MM, O'Malley MJ. Analysis and simulation of changes in EMG amplitude during high-level fatiguing contractions. *IEEE Trans Biomed Eng* 2003;50:1052–1062.
 27. Masuda K, Masuda T, Sadoyama T, Inaki M, Katsuta S. Changes in surface EMG parameters during static and dynamic fatiguing contractions. *J Electromyogr Kinesiol* 1999; 9:39–46.
 28. McGill KC, Dorfman LJ. High-resolution alignment of sampled waveforms. *IEEE Trans Biomed Eng* 1984;31:462–468.
 29. Merletti R, Knaflitz M, De Luca CJ. Myoelectric manifestations of fatigue in voluntary and electrically elicited contractions. *J Appl Physiol* 1990;69:1810–1820.
 30. Metting Van Rijn AC, Peper A, Grimbergen CA. Amplifiers for bioelectric events: a design with a minimal number of parts. *Med Biol Eng Comput* 1994;32:305–310.
 31. Naumann M, Reiners K. Diagnostic value of in situ muscle fiber conduction velocity measurements in myopathies. *Acta Neurol Scand* 1996;93:193–197.
 32. Ramaekers VT, Disselhorst-Klug C, Schneider J, Silny J, Forst J, Forst R, et al. Clinical application of a noninvasive multi-electrode array EMG for the recording of single motor unit activity. *Neuropediatrics* 1993;24:134–138.
 33. Stegeman DF, Linssen WHJP. Muscle fiber action potential changes and surface EMG: a simulation study. *J Electromyogr Kinesiol* 1992;2:130–140.
 34. Troni W, Doriguzzi C, Mongini T. Interictal conduction slowing in muscle fibers in hypokalemic periodic paralysis. *Neurology* 1983;33:1522–1525.
 35. Van Der Hoeven JH, Links TP, Zwarts MJ, Van Weerden TW. Muscle fiber conduction velocity in the diagnosis of familial hypokalemic periodic paralysis—invasive versus surface determination. *Muscle Nerve* 1994;17:898–905.
 36. Van Der Hoeven JH, Zwarts MJ, Van Weerden TW. Muscle fiber conduction velocity in amyotrophic lateral sclerosis and traumatic lesions of the plexus brachialis. *Electroencephalogr Clin Neurophysiol* 1993;89:304–310.